Adaptive Optics Scanning Laser Ophthalmoscope using a Micro-electro-mechanical (MEMS) Deformable Mirror

Yuhua Zhang, Siddharth Poonja, Austin Roorda
School of Optometry, University of California, Berkeley, CA 94720

ABSTRACT

A MEMS deformable mirror (DM)-based new generation adaptive optics scanning laser ophthalmoscope (AOSLO) has been developed for *in-vivo* microscopic imaging of the living human retina. With the miniaturized optical aperture of a μDMS-Multi™ MEMS DM made by Boston Micromachines Corporation (Watertown, MA), we were able to confine a compact and robust optical system to a mobile 30″×30″ breadboard while keeping the system aberrations diffraction-limited over an imaging field of view up to 3×3 degrees. A customized Shack-Hartmann wavefront sensor was devised to facilitate the MEMS DM based adaptive optics (AO) system. The ocular aberration is compensated over a 6mm pupil based upon a modal wavefront correction strategy. The AO correction is done for both ingoing and outgoing paths of the scanning laser ophthalmoscope. After AO correction, the root mean square wave aberration is reduced to less than 0.1μm for most eyes. The lateral resolution is effectively enhanced and the images reveal clear cone mosaic near the foveal center. The significant increase of the throughput at the confocal pinhole allows for a confocal pinhole whose diameter is less than the Airy disc of the collection lens, thereby fully exploiting the axial resolution capabilities of the system. The MEMS DM as well as its successful application represents the most significant technological breakthrough of this new generation AOSLO.

Key words: scanning laser ophthalmoscope; adaptive optics; micro-electro-mechanical systems; deformable mirror

1. INTRODUCTION

The development of the adaptive optics scanning laser ophthalmoscope (AOSLO) by Roorda et al.[1] marked a significant progress in ophthalmoscopy. The use of adaptive optics (AO) to correct the ocular aberrations of the human eye (which is the objective lens of the scanning laser ophthalmoscope[2] (SLO)) bestows the confocal SLO[3] with all the fundamental merits of a confocal scanning imaging mechanism such as enhanced resolution and fine optical sectioning ability. The merits of confocal imaging are very well treated by Webb[4], Roorda[5], Sheppard and Shotten[6] and Wilson and Sheppard[7]. The first AOSLO produced microscopic real-time views of the living human retina with unprecedented optical quality. It yielded the first real-time images of photoreceptors and blood flow in the human retina at video rates, which facilitates many promising applications in revealing retinal disease mechanisms[8,9], improving diagnosis[10] and SLO psychophysics[11]. The AOSLO has become an attractive microscopic imaging modality for living human eye.

AO has proved to be an indispensable mechanism for high quality ophthalmic optical imaging[12-15] and the DM plays the key role in realization of an effective and efficient AO system. The first AOSLO employed a 37-channel mechanical DM (Xinetics Inc., Devens, MA), which has a continuous mirror face sheet offering a 46mm effective optical aperture

Ophthalmic Technologies XVI, edited by Fabrice Manns, Per G. Söderberg, Arthur Ho,
Proc. of SPIE Vol. 6138, 61380Z, (2006) · 1605-7422/06/$15 · doi: 10.1117/12.646934

that is fixed to an array of individually addressable, discrete piezoelectric actuators. In order to map the human pupil to the effective aperture of the DM, relay telescopes with large magnification ratios had to be applied thus leading to a fairly large overall system structure which occupied about 1.5m×1m area on an optical table[1]. The DM performed very well but with a high cost and large size.

The evolution and use of AO systems for visual optics is paralleled by the progress and manufacturing technology of DMs. Dreher et al.[16] used a 13-segment DM to compensate the astigmatism of the eye. Liang et al.[13] successfully employed a mechanical DM (Xinetics, Andover, MA) of 37 channels over 46mm aperture with lead zirconate-titanate (PZT) actuators to correct high order ocular aberration. Based on the Liang et al. system, Hofer et al.[17] realized a close-loop dynamic AO retinal imaging system and further improved the imaging quality with a Xinetics lead magnesium niobate (PMN) DM. Fernandez et al.[18] and Hermann et al.[19] employed 37-channel micromachined membrane DMs (OKO Technologies, Holland). Vargas-Martin et al.[20] exploited a transmissive liquid-crystal spatial light modulator. More recently, Doble et al.[21,22] reported their exploration of a prototype microelectromechanical (MEMS) DM (Boston Micromachines Co., Boston, MA) for AO in the human eye. Judged by the actuator density, the maximum stroke, the response speed, the compactness as well as the potentially low cost, the MEMS DM demonstrates significant advantages in building a robust AO system, and represents the most promising technology. Boston Micromachines Co. (BMC) has pushed the MEMS DM from prototype to real product[23,24] that, to a reasonable degree, meets the requirements for an effective AO system for vision applications[25-27].

Encouraged by the results of the first AOSLO and the progress of the MEMS DM manufacturing technology, a new generation AOSLO is being developed aimed at better compensation of the wave aberrations of the eye thereby rendering higher-quality microscopic views of the living retina, all housed in a compact structure that is clinically deployable.

In this paper, we present the development and imaging results of the new AOSLO that uses the cutting-edge MEMS DM.

2. METHODS

2.1. AOSLO Optical System

Shown in Fig.1 is the general system of the new generation AOSLO. The light from the tip of a single mode fiber is collimated by lens L1 and is relayed by the telescope which is constituted by L2, L3 and the beam splitter (BS) to the DM, the HS, the VS, and finally to the eye where it scans to form a raster pattern on the retina. The diffusely reflected light from the retina transmits inversely along the ingoing path to the VS, HS, DM and to the beam splitter, where most of the light passes through and is relayed by a telescope, constituted by L4-L5, to the collection lens L6. A confocal pinhole is placed at the focal point of the collector lens. The signal is received by the photo detector and is acquired and processed by the computer for storage and display. The optical system occupies about 0.5m×0.5m area on a mobile

optical work table while keeping the system aberrations diffraction-limited over an imaging field up to 3×3 degrees. Shown in Fig.2 are the spot diagrams of the scanning optical system at 9 points over its 3 degree scanning field.

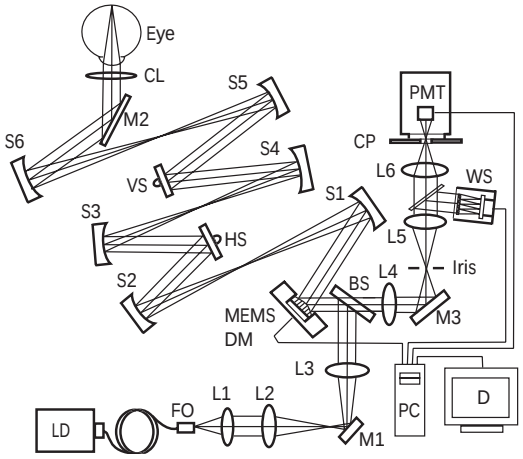

Fig.1. LD, laser diode; FO, fiber output; PC, computer; D, display; BS, beam splitter; HS, horizontal scanner (16KHz); VS, vertical scanner (30, 60 Hz); CL, cylindrical lens; WS, wavefront sensor; CP, confocal pinhole; PMT, photomultiplier tube; M1~M3, flat mirrors; S1~S6, spherical mirrors; L1~L6, achromatic lenses.

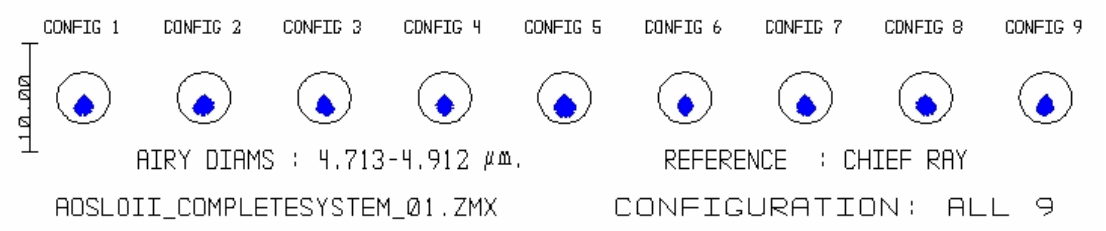

Fig.2. AOSLOII scanning optics configuration matrix spot diagram

2.2. MEMS DM based AO

The MEMS DM is the µDMS-Multi™ made by Boston Micromachines Corporation (Watertown, MA), which consists of a single membrane supported by an underlying actuator array. Deflection of the mirror surface is via electrostatic attraction, and each actuator is individually addressable. Although this DM has a continuous membrane reflecting surface, it differs from a conventional membrane design. Cross-talk between actuators is minimized by constructing the actuator array with a double cantilever design. The mirror is described in detail elsewhere[23, 24]. The specific mirror array is a 140 actuator design (12 X 12 with no corner actuators) over a 4.4 mm clear aperture. The actuator stroke is 3.5 microns.

A Shack-Hartmann wavefront sensor was built to facilitate the AO system. The lenslet array has a 0.328mm×0.328mm pitch with a 24mm focal length. By scanning a diffusely scattering surface through the focal point of a model eye, we calibrated the wavefront sensor. The result is shown in Fig.3.

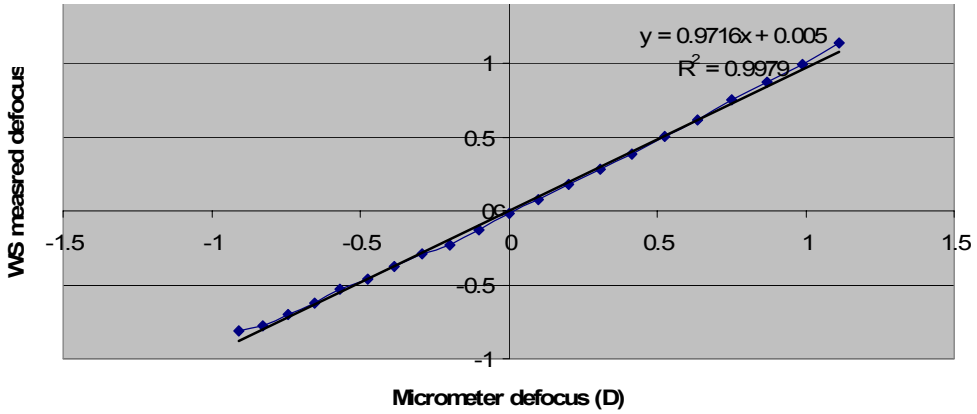

Fig.3. AOSLO wavefront sensor calibration

The DM, the lenslet array of the Shack-Hartmann wavefront sensor, the HS, VS, the pupil plane of the eye and the collection lens are designed and delicately aligned such that they conjugate to each other. The wavefront is corrected for both ingoing and outgoing path.

A modal approach is adopted to run the AO closed loop. A 10^{th} order Zernike polynomial is fitted to the wavefront slopes. The actuator deflections are then calculated directly from the best fit wavefront. We adopted a proportional control strategy and achieved a closed-loop update frequency of about 10 Hz.

2.3. Light Sources and Imaging Acquisition

Two light sources are currently used in the MEMS DM based AOSLO for different scientific purposes. One is a common diode laser with a wavelength of 655nm and the other one is an 840 nm low-coherence superluminescent laser diode (SLD) (Broadlighter S840-HP, Superlum, Russia), which is used to reduce interference artifacts and speckle in the images[30]. A photomultiplier tube (Hamamatsu, Japan) is employed to detect the signal photons that pass through the confocal pinhole. A frame grabber digitizes pixels at a 20 MHz detection rate to generate 8-bit 512×512 frames at 30 frames per second.

2.4. Imaging Protocol

In practice, the human eyes were dilated (one topically applied drop each of 0.5 % tropicamide and 2.5 % phenylephrine) and the correction was done over a 6mm pupil. Approvals for image human subjects were obtained by the University of California, Berkeley IRB, and informed consent was obtained from each subject prior to imaging.

Before running AO, we first used trial lenses to minimize the defocus and astigmatism so that we would not saturate the DM actuators. When the 655nm diode laser is used, the illumination power at the cornea is 60μw, which is about 1/50th of what the ANSI standard considers to be safe exposure levels[32]. Whereas for the 840nm SLD, the illumination power is 300μw, which is also far below the safety exposure level at this wavelength.

3. RESULTS

More than 10 human subjects including several with eye diseases have been imaged. The AO reduced the root mean square wave aberration over a 6 mm pupil from 0.4μm to less than 0.1μm.

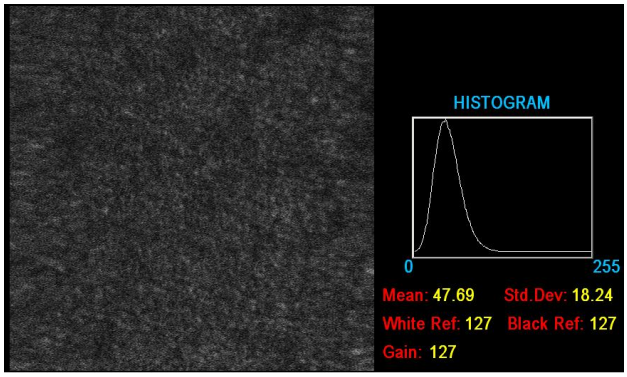

(a)

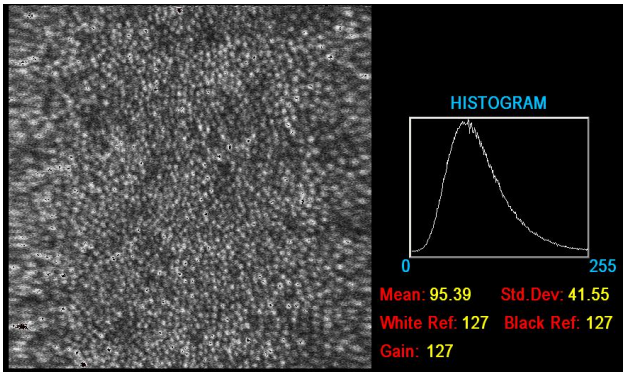

(b)

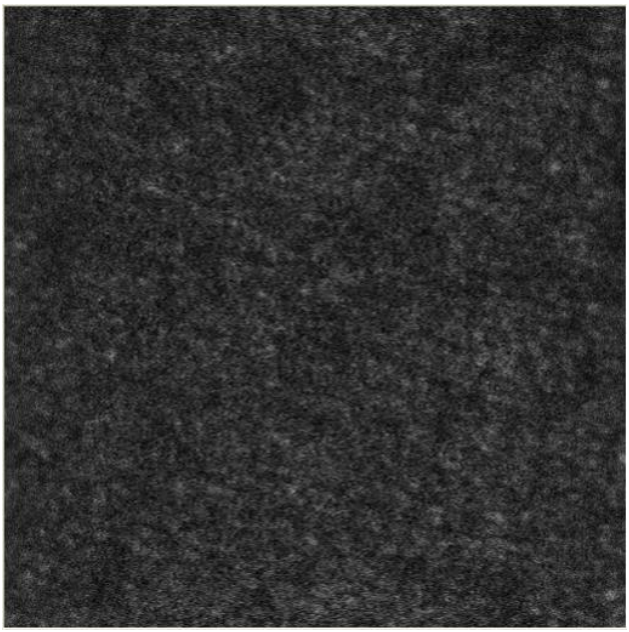

(c)

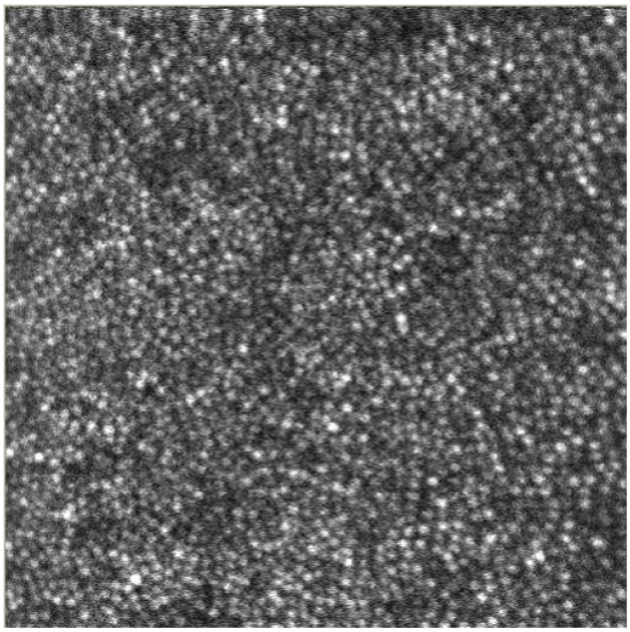

(d)

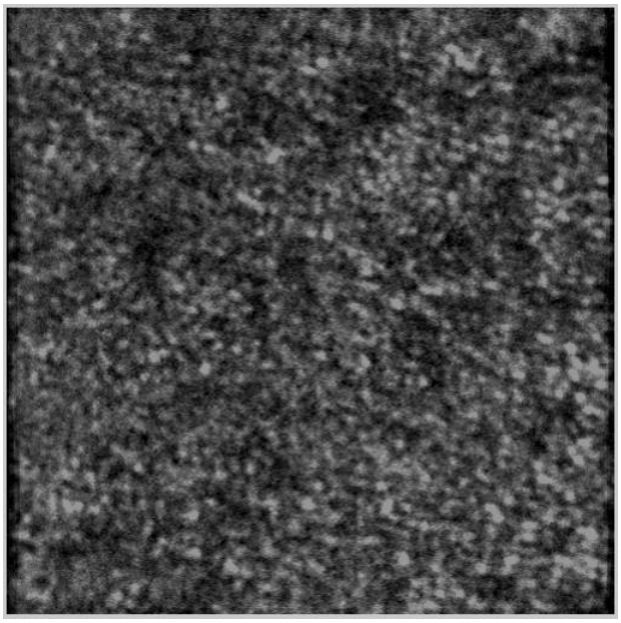

(e)

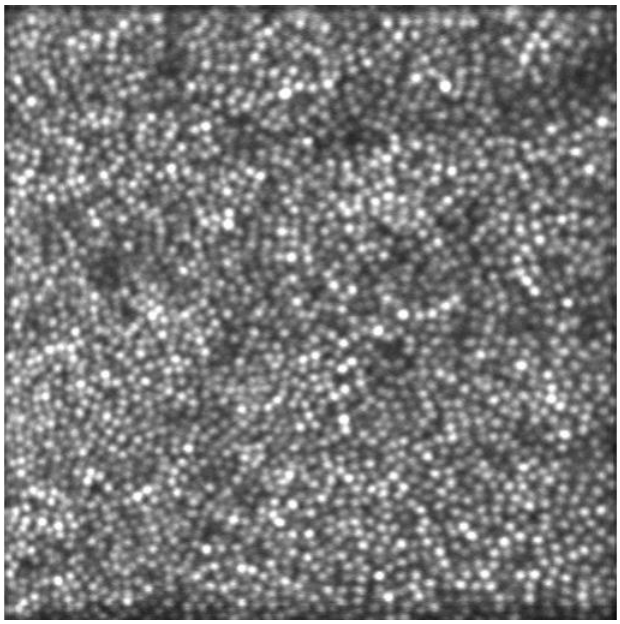

(f)

Fig.4. (a) is a screen-shot of a single frame from the real-time imaging monitor, which was taken before AO correction but after best correction of defocus and astigmatism with trial lenses. A real-time histogram was programmed to display the statistical characteristics of each single frame. Frame (b) was taken after AO correction. (c) and (d) show the corresponding frames of (a) and (b) after correction of the distortion generated by the sinusoidal scan pattern of the horizontal scanner. (e) and (f) are registered images of 10 frames before and after AO correction, respectively. These images were from a retinal area about 1^0 eccentricity from the foveal center. The field of view is 1.2^0. The registered images have been corrected for distortions due to eye movements[31]. These images were obtained with the 840nm SLD

Fig.4 shows retinal images from one subject before and after AO correction. The AO correction demonstrates the threefold benefit of increased brightness, improved contrast and enhanced lateral resolution of the images.

Shown in Fig.5(a)~Fig.5(e) are a series of images of another subject's eye. Each image spans a 1.2×1.2 degree field of view. The images were taken with the 840nm SLD light source. Fig.5(f) is a composite made by stitching together a series of frames spanning about a 5.2×5.2 degree field of view. The squares indicate the positions of Fig.5(a)~Fig.5(e) on the retina. O indicates the foveal center. Except for the very central 0.5 degree field at the foveal center, the images show a well resolved and contiguous cone mosaic.

The robustness of the MEMS DM based AO is also demonstrated by its formation of a very compact focused spot at the confocal pinhole via the collection lens. This enables us to use smaller pinholes while maintaining a decent signal to noise ratio for imaging. Moreover, with smaller pinhole, the AOSLO has better axial resolution[28, 29]. Fig.6(a)~Fig.6(c) show the images that were obtained from the same retinal area of a subject using 75μm, 50μm and 25μm pinhole,

respectively. We need note that the 25μm pinhole is only 0.833 times of the Airy disc diameter of the collection optics (655nm wavelength laser, beam diameter is 5.4mm, collection lens focal length is 100mm focal length). Fig.6(d) illustrates the improvement of the axial discrimination capability with the decrease of the pinhole size as measured by moving a diffusely scattering plane through the focal plane of a model eye.

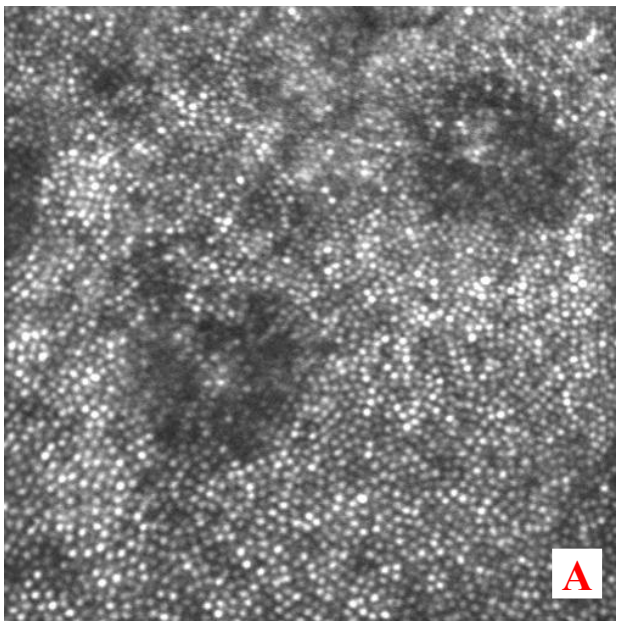

(a)

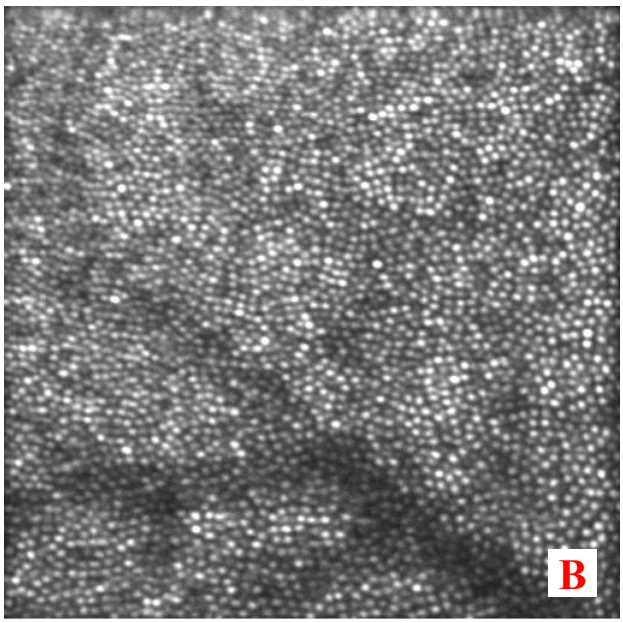

(b)

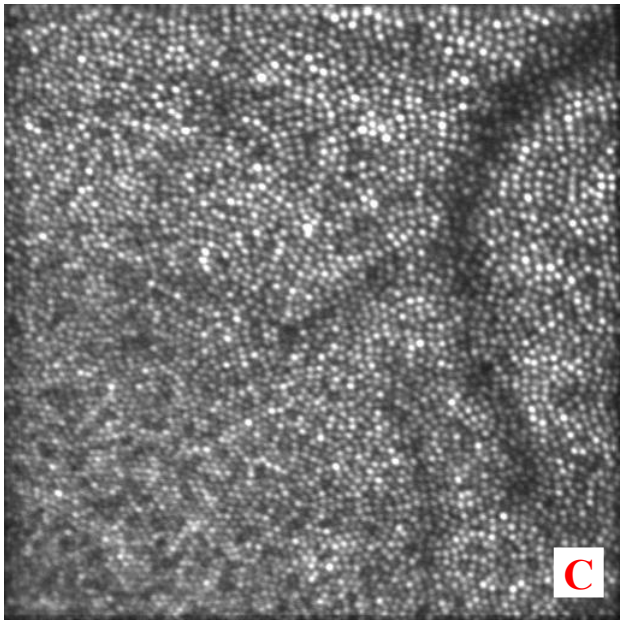

(c)

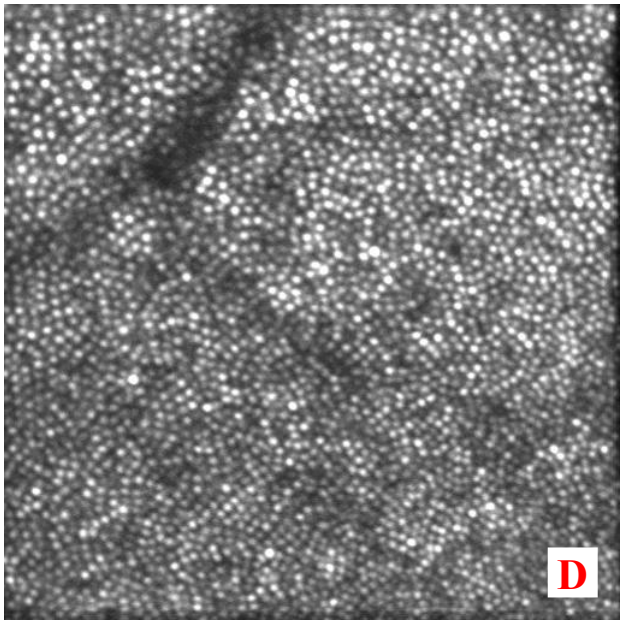

(d)

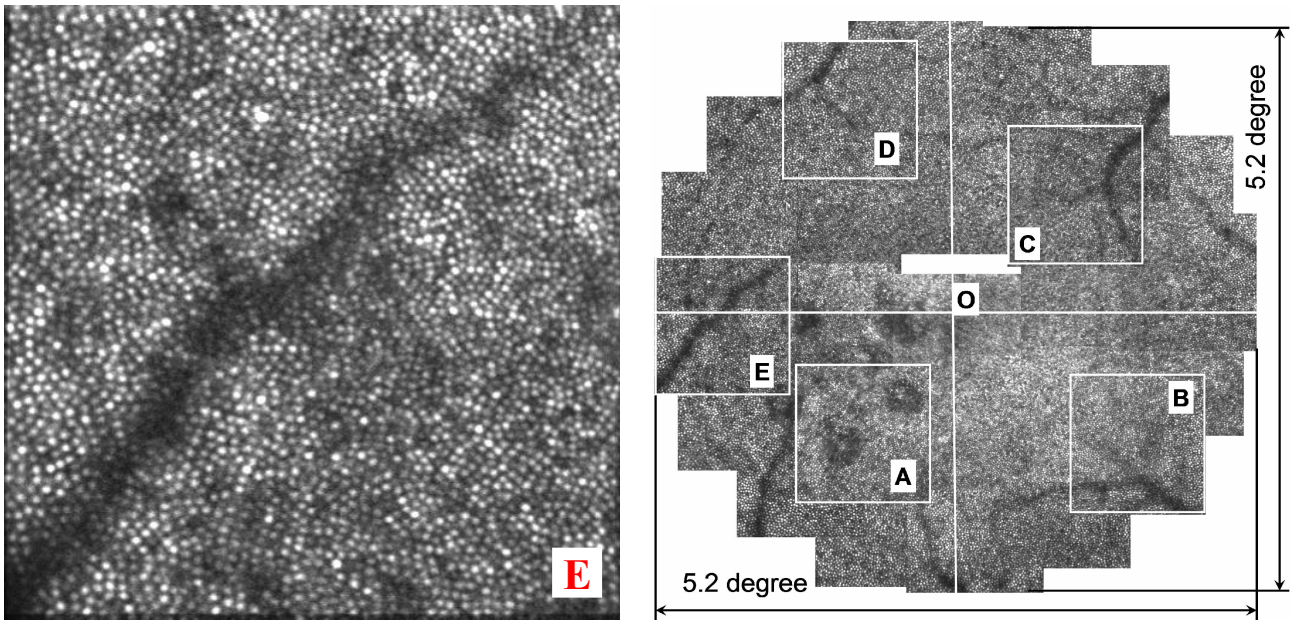

(e) (f)

Fig.5 Foveal cone mosaic images obtained with the AOSLO

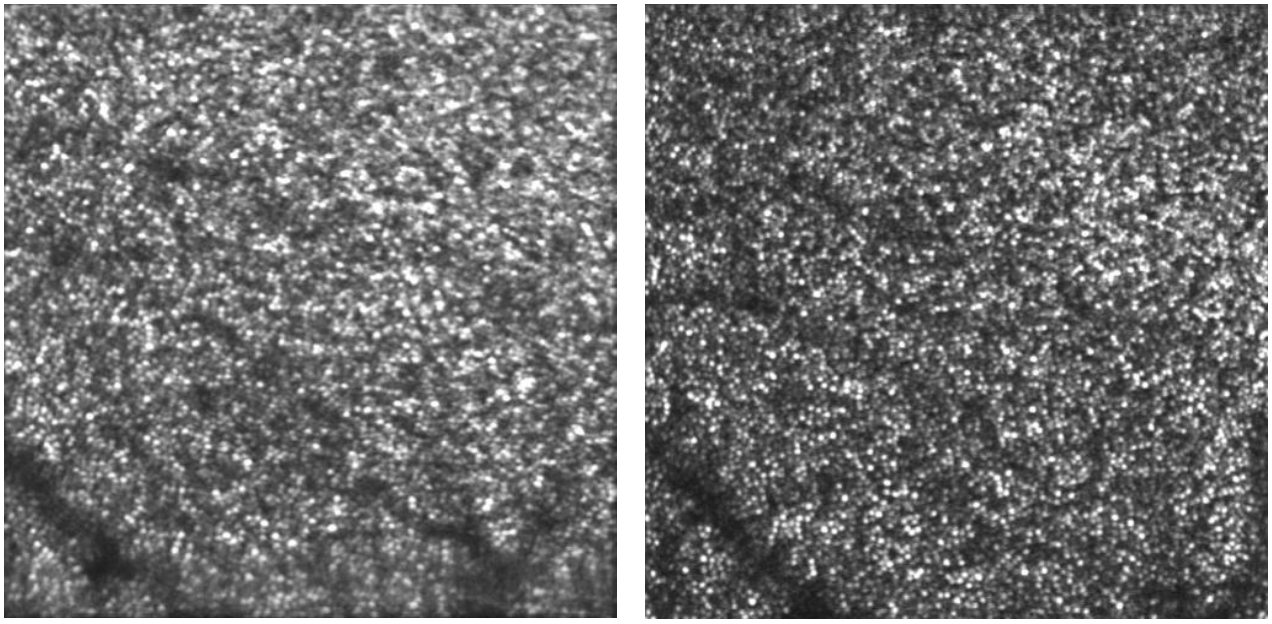

(a) (b)

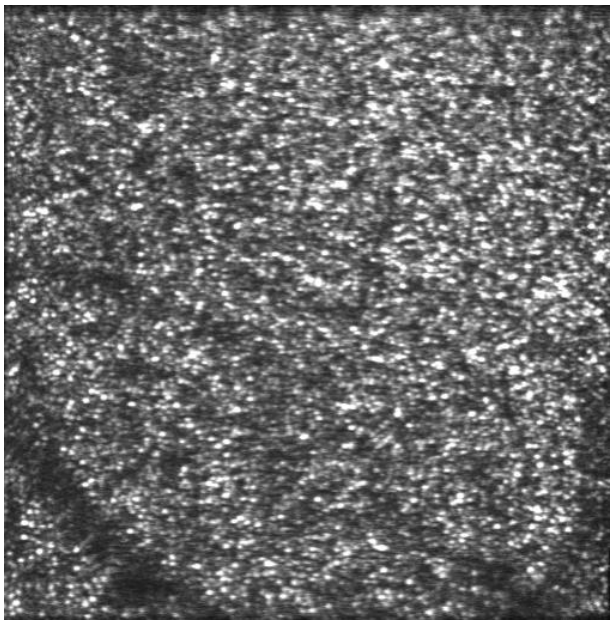

(c)

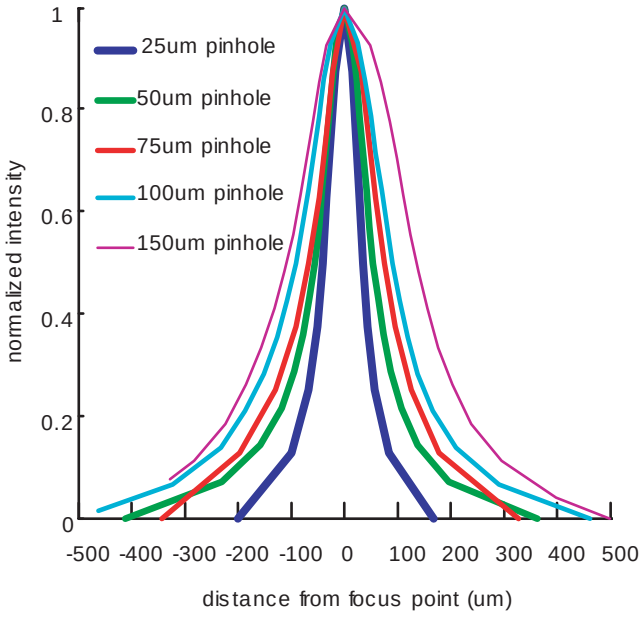

(d)

Fig.6, (a), (b) and (c) are the same retinal area taken with 75μm, 50μm and 25μm pinhole, respectively. They are from a location about 1^0 eccentricity from the foveal center and have a field of view of 1.5^0. These images were obtained with the 655nm diode laser. (d) is the measured axial intensity distribution through the focus with pinholes of different diameters.

4. CONCLUSION

We have developed a compact and robust MEMS DM based AOSLO, which takes advantage of the cutting-edge technology of the MEMS DM. We have obtained real-time images of microscopic structures in the living human retina and have achieved correction levels that are comparable, and often better, than those that obtained in our first generation AOSLO which uses a 37 element discrete actuator deformable mirror (Xinetics, Inc).

ACKNOWLEDGEMENTS

This work is funded by the NIH Bioengineering Research Partnership grant EY014365 and the National Science Foundation Science and Technology Center for Adaptive Optics, managed by the University of California, Santa Cruz under cooperative agreement #AST-9876783.

REFERENCES:

1. A. Roorda, F. Romero-Borja, W. J. Donnelly, H. Queener, T. J. Hebert and M. C. W. Campbell, "Adaptive optics scanning laser ophthalmoscopy", Optics Express **10**, 405-412, 2002.

2. R. H. Webb and G. W. Hughes, “Scanning laser ophthalmoscope”, IEEE Trans. Biomed. Eng., **28**, 488–492, 1981.
3. R. H. Webb, G. W. Hughes, and F. C. Delori, "Confocal scanning laser ophthalmoscope", Appl.Opt., **26**, 492-1499, 1987.
4. R.H. Webb, “Confocal optical microscopy”, Reports on Progress in Physics, **59**, 427 – 451, 1996.
5. A. Roorda, *Double Pass Reflections in the Human Eye*, Ph.D. thesis, University of Waterloo, Waterloo, Ontario, Canada, 1996.
6. C.J.R. Sheppard and D.M. Shotton, *Confocal microscopy*, Springer-Verlag New York Inc., New York, 1997.
7. T. Wilson and C. J. R. Sheppard, *Theory and Practice of Scanning Optical Microscopy*, Academic Press, London, 1984.
8. J.A. Martin and A. Roorda, “Direct and non-Invasive assessment of parafoveal capillary leukocyte velocity”, Ophthalmology, **112**, 2219-2224, 2005.
9. A. S. Vilupuru, N.V. Rangaswamy, L.J. Frishman, R.S. Harwerth, and A. Roorda, “Adaptive optics ophthalmoscopy for imaging of the lamina cribrosa in glaucoma,” Invest. Ophthalmol. Vis. Sci., **46**: E-Abstract, 3515, 2005.
10. J. I. Wolfing, M. Chung, J. Carroll, A. Roorda, S. Poonja, A.S. Vilupuru, and D.R. Williams, “High resolution imaging of cone–rod dystrophy with adaptive optics,” Invest. Ophthalmol. Vis. Sci., **46**: E-Abstract, 2567, 2005.
11. S. Poonja, S. Patel, L. Henry, A. Roorda. “Dynamic visual stimulus presentation in an adaptive optics scanning laser ophthalmoscope”, Journal of Refractive Surgery, **21**, 575-580, 2005.
12. A. Roorda and D. R. Williams, "The arrangement of the three cone classes in the living human eye", Nature, **397**, 520-522, 1999.
13. J. Liang, D. R. Williams, and D. T. Miller, ‘‘Supernormal vision and high-resolution retinal imaging through adaptive optics’’, J. Opt. Soc. Am. A, **14**, 2884–2892, 1997.
14. D.R. Williams, J. Liang, D.T. Miller, and A. Roorda, "Wavefront Sensing and Compensation for the Human Eye", Chap.10 in *Adaptive Optics Engineering Handbook*, R. K. Tyson, Eds., pp.287-310, Marcel Dekker, New York, 2000.
15. J. Carroll, M. Neitz, H. Hofer, J. Neitz, and D. R. Williams. "Functional photoreceptor loss revealed with adaptive optics: an alternate cause of color blindness", Proc. Natl. Acad. Sci. U.S.A , **101**, 8461-8466, 2004.
16. A. W. Dreher, J. F. Bille, and R. N. Weinreb, ‘‘Active optical depth resolution improvement of the laser tomographic scanner’’, Appl. Opt., **28**, 804–808, 1989.
17. H. Hofer, L. Chen, G. Y. Yoon, B. Singer, Y. Yamauchi, and D. R. Williams, “Improvement in retinal image quality with dynamic correction of the eye’s aberration”, Optics Express, **8**, 631-643, 2001.
18. E. J. Fernandez, I. Iglesias and P. Artal, “Closed-loop adaptive optics in the human eye”, Opt. Lett., **26**, 746-748, 2001.
19. B. Hermann, E. J. Fernandez, A. Unterhuber, H. Sattmann, A. F. Fercher, W. Drexler, P. M. Prieto, and P. Artal., “Adaptive-optics ultrahigh-resolution optical coherence tomography”, Opt. Lett., **29**, 2142-2144, 2004.

20. F. Vargas-Martin, P. M. Prieto, and P. Artal, "Correction of the aberrations in the human eye with a liquid-crystal spatial light modulator: limits to performance", J. Opt. Soc. Am. A **15**, 2552-2562. 1998.
21. N. Doble, G. Yoon, P. Bierden, L. Chen, S. Olivier, and D. R. Williams, "Use of a microelectromechanical mirror for adaptive optics in the human eye", Optics Lett., **27**, 1537-1539. 2002.
22. N. Doble and D. R. Williams, "The application of MEMS technology for adaptive optics in vision science", IEEE Journal of Selected Topics in Quantum Electronics, **10**, 629-635, 2004.
23. T. G. Bifano, J. A. Perreault, P. A. Bierden, and C. E Dimas, "Micromachined deformable mirrors for adaptive optics," in *High Resolution Wavefront Control: Methods, Devices, and Applications IV*, J. D. Gonglewski, M. A. Vorontsov, M. T. Gruneisen, S. R. Restaino, and R. K. Tyson, eds. Proceedings of SPIE **4825**, 10-13. SPIE, Bellingham, WA, 2002.
24. J. A. Perreault, T. G. Bifano, B. M. Levine and M. Horenstein, "Adaptive optic correction using microelectromechanical deformable mirrors", Optical Engineering, **41**, 561-566, 2002.
25. N. Doble and D. T. Miller, "Wavefront Correctors for Vision Science," in *Adaptive Optics for Vision Science: Principles, Practice, Design and Applications*, J. Porter, A. Awwal, J. Lin, H. Queener, and K. Thorn, eds. Wiley & Sons, **in press.**
26. J. Porter, A. Guirao, I. G. Cox, and D. R. Williams, "Monochromatic aberrations of the human eye in a large population", J. Opt. Soc. Am. A, **18**, 1793-1803, 2001.
27. L. N. Thibos, X. Hong, A. Bradley, and X. Cheng, "Statistical variation of aberration structure and image quality in a normal population of healthy eyes", J. Opt. Soc. Am. A, **19**, 2329-2348, 2002.
28. T. Wilson, ''The role of the pinhole in confocal imaging systems,'' Chap. 11 in *The Handbook of Biological Confocal Microscopy*, 2dn Edition, J. B. Pawley, Eds., pp. 167–182, Plenum, New York, 1995.
29. K. Venkateswaran, F. Romero-Borja and A. Roorda. "Theoretical Modeling and Evaluation of the Axial Resolution of the Adaptive Optics Scanning Laser Ophthalmoscope," J. Biomed. Opt. 9: 132-138, 2004.
30. A. Roorda and Y. Zhang. "Mechanism for cone reflectance revealed with low coherence AOSLO imaging," Invest.Ophthalmol.Vis.Sci. 46, E-Abstract 2433. 2005.
31. C. R. Vogel, D. Arathorn, A. Roorda, and A. Parker, "Retinal motion estimation and image dewarping in adaptive optics scanning laser ophthalmoscopy", Optics Express, **in press**.
32. *American National Standard on the Safe use of Lasers*, ANSI Z136.1-2000, American National Standards Institute, 2000.